ARTICLES

Intramolecular Energy Transfer in Fullerene Pyrazine Dyads

Dirk M. Guldi*

Radiation Laboratory, University of Notre Dame, Notre Dame, Indiana 46556

G. Torres-Garcia[†] and J. Mattay[‡]

Institut für Organische Chemie der Universität Kiel, D-24098 Kiel, Germany

Received: April 16, 1998; In Final Form: July 7, 1998

Excited-state properties of three different pyrazine derivatives **4**−**6** were probed by emission and transient absorption spectroscopy. They display emission maxima at 464 (**4**), 417 (**5**), and 515 nm (**6**) that are red-shifted with respect to their strong UV ground-state absorption and formed with overall quantum yields (Φ) of 0.156, 0.22, and 0.13, respectively. Once photoexcited, these triplet excited pyrazines undergo rapid intermolecular energy transfer to a monofunctionalized fullerene derivative (**7**) with bimolecular rate constants ranging from 3.64×10^9 M^{-1} s^{-1} (**6**) to 1.1×10^{10} M^{-1} s^{-1} (**4**). The product of these bimolecular energy-transfer reactions is in all cases the fullerene triplet excited state. Functionalization of pristine C_{60} with the investigated pyrazine derivatives promotes the UV−vis absorption characteristics and, in turn, improves the light-harvesting efficiency of the resulting dyads **1**−**3** relative to pristine C_{60}. Photoexcitation of the pyrazine moieties in dyads **1**−**3** leads to the formation of their singlet excited states. In contrast to the pyrazine models, photoexcitation of dyad **1**−**3** is followed by rapid intramolecular deactivation processes of the latter via energy transfer to the fullerene ground state with half-lives between 37 and 100 ps. In turn, energy transfer transforms the short-lived and moderately redox-active singlet excited states of pyrazine into the highly reactive fullerene triplet excited state. The latter is found to produce effectively singlet oxygen ($^1O_2$) with quenching rate constants for **1**−**3** of $(1-1.5) \times 10^9$ M^{-1} s^{-1}. Similarly, reductive quenching of the triplet excited states in dyads **1**−**3** via electron transfer with diazabicyclooctane (DABCO) occurs with rate constants of $(5.2-9.4) \times 10^7$ M^{-1} s^{-1}.

Introduction

The remarkable electron and energy acceptor properties of pristine fullerenes evoked a lively interest in employing them in bimolecular transfer reactions performed in homogeneous solutions[1−7] or across biologically relevant membrane interfaces.[8−11] This unique reactivity, in combination with the predominantly hydrophobic nature of C_{60}, led to the development of versatile methodologies aimed at the modification of its polyfunctional structure.[12−17] Covalent attachment of a large number of addends across the double bonds located at the junctions of two hexagons afforded novel and innovative materials with appealing characteristics ranging from drug delivery to advanced electronic devices.[15,18,19]

Among those materials, donor−acceptor superstructures with electroactive or photosensitive addends are of particular importance.[15,18] In ferrocene (Fc)[20,21] or dimethylaniline (DMA)[22−24] based multicomponent supermolecules, fullerenes were implemented as photosensitizers that undergo intramolecular electron-transfer processes. Chromophore units, such as porphyrins or ruthenium complexes, synthetically bound to the C_{60} core changed the role of the fullerene.[25−32] In these cases, fullerenes were found to operate exclusively as electron-accommodating acceptor moieties. A particular sensitive set of parameters for the study of electronic properties and excited-state interactions of these fullerene-containing dyads are optical absorption and emission spectra.

Reports on intramolecular energy-transfer reactions to fullerenes are relatively scarce.[33] Energy-transfer processes in a cascadelike arrangement are the focus of efficient light conversion into states that are longer-lived than the precursor excited state. An alternative motivation is the biologically important production of singlet oxygen ($^1O_2$) as a product of excited-state quenching.[1,3] The fullerene's excellent capability of generating singlet oxygen in high yields suggests, for example, their potential use in antitumor activity.[19]

In light of the fullerene's moderate absorption features in the visible, where human tissues are relatively transparent, incorporation of additional photosensitizers is an important objective. Suitable photosensitizers assist in extending the absorption further into the red and transfering their excited-state energy. Covalent functionalization of pristine C_{60} with the envisaged pyrazine moieties would enhance the ground-state absorption of the resulting dyads and is expected to promote the light-

* To whom correspondence should be addressed. E-mail: GULDI@MARCONI.RAD.ND.EDU.

[†] Permanent Address: University of Malaga, Spain.

[‡] New Address: Organische Chemie I, Fakultät für Chemie, Universität Bielefeld, Postfach 100131, D-33501 Bielefeld, Germany.

10.1021/jp9818885 CCC: $15.00
Published on Web 10/29/1998

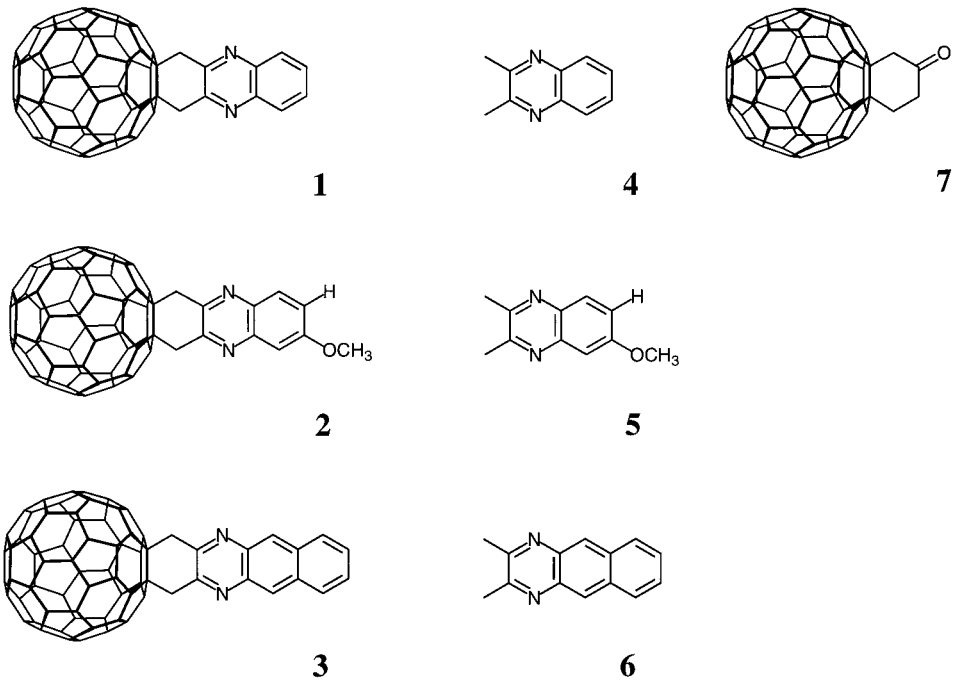

Figure 1. Compounds used in this study.

harvesting effect. We have chosen the pyrazine substituent not only because it is often used as a chromophor of azine dyes[34] but also because of its occurrence as a natural pigment.[35] In addition, pyrazine and quinoxaline derivatives play an important role in medicinal chemistry, for example, as antibiotics.[36] The focus of the present study is to probe these systems in photoinduced transient spectrophotometric studies and to quantitate the dynamics and efficiency of intramolecular energy-transfer processes.

Experimental Section

Details of the synthesis of fullerene dyads **1**−**3** and pyrazine model compounds **4**−**6** are described elsewhere (Figure 1).[37] Monofunctionalized fullerene derivative **7** was purchased from MER (Tucson, AZ).

Picosecond laser flash photolysis experiments were carried out with 355 nm laser pulses from a mode-locked, Q-switched Quantel YG-501 DP Nd:YAG laser system (pulse width of ∼18 ps, 2−3 mJ/pulse). The white continuum picosecond probe pulse was generated by passing the fundamental output through a D_2O/H_2O solution. The excitation and the probe was fed to a spectrograph (HR-320, ISDA Instruments, Inc.) with fiberoptic cables and were analyzed with a dual diode array detector (Princeton Instruments, Inc.) interfaced with an IBM-AT computer. Picosecond kinetic time−absorption profiles represent an average wavelength region taken over ca. 10 nm. Nanosecond laser flash photolysis experiments were performed with laser pulses from a Molectron UV-400 nitrogen laser system (337.1 nm, 8 ns pulse width, 1 mJ/pulse) in a front-face excitation geometry.[38]

Pulse radiolysis experiments were accomplished using 50 ns pulses of 8 MeV electrons from a model TB-8/16-1S electron linear accelerator. Basic details on the equipment and the data analysis have been described elsewhere. Dosimetry was based on the oxidation of SCN^- to $(SCN)_2^{\bullet -}$, which, in N_2O-saturated aqueous solutions, takes place with $G \approx 6$ (G denotes the number of species per 100 eV, or the approximate micromolar concentration per 10 J of absorbed energy). The radical concentration generated per pulse amounts to $(1-3) \times 10^{-6}$ M for all systems investigated in this study.

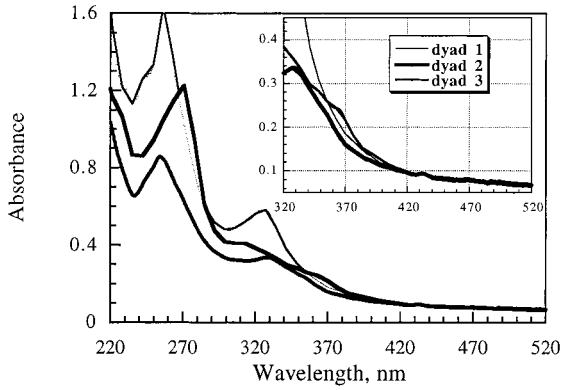

Figure 2. Room-temperature UV−vis spectra of dyads **1**−**3** in methycylcohexane.

Absorption spectra were recorded with a Milton Roy Spectronic 3000 array spectrophotometer. Emission spectra were recorded on a SLM 8100 spectrofluorometer. Fluorescence spectra of derivatives **1**−**7** were measured in methylcyclohexane (5.0×10^{-5} M), which forms a clear, noncracking glass at liquid nitrogen temperature. The excitation wavelength was adjusted to the pyrazine's ground-state absorption (**4**, 380 nm; **5**, 342 nm; **6**, 377 nm). A 570 nm long-pass filter in the emission path was used in order to eliminate the interference from the solvent and stray light. Long integration times (20 s) and low increments (0.1 nm) were applied. The slits were 2 and 8 nm. Each spectrum was an average of at least five individual scans.

Results and Discussion

Absorption Spectra. The ground-state absorption spectra of fullerene dyads **1**−**3** in methylcyclohexane reveal superimposed characteristics of both chromophore moieties, namely, the fullerene core and the pyrazine functionalities (see Figure 2). Pyrazine model **6** in methylcyclohexane, for example, absorbs strongly around 270 nm followed by maxima at 311(sh), 330, 345, 361, 377, 400, 450, and 472 nm. In contrast,

TABLE 1: Absorption Maxima of Dyads 1−3, Pyrazine Models 4−6, and Fullerene Model 7 in Methylcyclohexane

compound	absorption maxima [nm][a]
dyad **1**	243, *256*, *311*, 325, 380, *433*, *531*, *622*, *634*, *653*, *666*, *677*, *687*, *699*
dyad **2**	244, *255*, *328*, 353(sh), *433*, *531*, *622*, *634*, *653*, *666*, *677*, *687*, *699*
dyad **3**	*255*, 271, *309*, 330(sh), 345(sh), 362, 394, *433*, 450, *531*, *622*, *634*, *653*, *666*, *677*, *687*, *699*
pyrazine **4**	380
pyrazine **5**	331, 342
pyrazine **6**	270, 311(sh), 330, 345, 361, 377, 400, 450
fullerene **7**	*256*, *311*, *433*, *531*, *622*, *634*, *653*, *666*, *677*, *687*, *699*

[a] Italic numbers indicate fullerene-related absorption; all other numbers indicate pyrazine-related absorption.

fullerene **7**, which, because of its structural similarity to dyads **1**−**3**, serves as a fullerene model throughout the course of this study, shows absorption at *255*, *308*, and *433* nm (note that the fullerene absorptions are listed in italic font). Dyad **3**, carrying both a fullerene and a pyrazine unit, shows a set of absorption maxima in the UV−vis range at *255*, 271, *309*, 330(sh), 345 (sh), 362, 394, *433*, 450, and 472 nm. Furthermore, a set of multiple absorption bands with maxima at *622*, *634*, *653*, *666*, *677*, *687*, and *699* nm can be taken as spectral evidence that substantiates the partially broken C_{2v} symmetry of the fullerene core in dyad **3** relative to pristine C_{60} (I_h). The absorption maxima of dyads **1** and **2** and their spectral assignments are summarized in Table 1. The strictly superimposed absorption features of the pyrazine and fullerene centers in dyads **1**−**3** exclude formation of additional charge-transfer bands and, in fact, suggests insignificant electronic ground-state interactions.

Steady-State Emission. Emission spectroscopy is a powerful tool that can be employed to obtain detailed information on excited-state energies and lifetimes of emitting species. Accordingly, deactivation of excited states, such as electron and energy-transfer processes with carefully chosen acceptors, is probed by following emission quantum yields.

The excited states of pyrazine models **4**−**6** emit strongly in the 400−600 nm range with quantum yields (Φ) of 0.156, 0.22, and 0.13, respectively. Their emission maxima at 464, 417, and 515 nm correspond to excited-state energies of 2.67 eV (**4**), 2.97 eV (**5**), and 2.41 eV (**6**) (Figure 3a). In contrast, fullerene−pyrazine dyads **1**−**3** show strongly quenched emission ($\Phi \approx 3.0 \times 10^{-4}$) in this region upon irradiation to give the respective pyrazine ground-state transitions (Figure 3b). This points to efficient deactivation of the photoexcited pyrazine moieties by intramolecular quenching.

The fullerene's fluorescence in dyads **1**−**3**, with strong ($^*S_0 \rightarrow S_0$) transitions around 701 nm and $\Phi_{Fl} = 6.0 \times 10^{-4}$, remained, however, unaffected relative to fullerene model **7** (Table 2 and Figure 3).[39] In addition, the emission spectra gave rise to a weak phosphorescence peak at 826 nm. The low phosphorescence quantum yield, relating to the emission from the fullerene triplet excited state, prevents meaningful conclusions in view of possibilities of energy transfer from the photoexcited pyrazine. In particular, helping to resolve whether the implied intramolecular dynamics may lead to the generation of the fullerene's excited singlet or triplet state.

In conclusion, studies regarding the emission of dyads **1**−**3** demonstrate that rapid quenching of the electronically excited pyrazines gives rise to only a single emitting species, namely, the fullerene moiety.

Time-Resolved Transient Spectroscopy. The rapid deactivation of the photoexcited pyrazine centers in dyads **1**−**3** points to their effective interactions with the fullerene moieties. Pico- and nanosecond-resolved photolysis are important spectroscopic techniques for characterizing dynamic processes that are associated with the generation and fate of photoexcited states and, thus, to complement the emission studies.

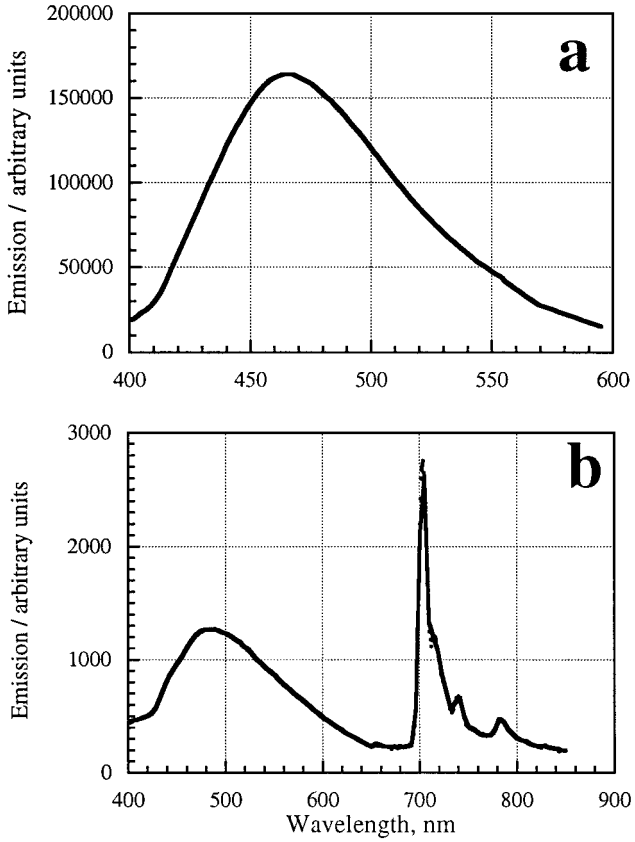

Figure 3. Emission spectra (a) of pyrazine model **4** (5.0×10^{-5} M) and (b) dyad **1** (5.0×10^{-5} M) in methylcylcohexane at 77 K (excitation at 380 nm).

TABLE 2: Emission Maxima of Dyads 1−3 and Fullerene Model 7 in Methylcyclohexane

compound	fluorescence maxima [nm][a]
dyad **1**	(464)[b] 701, 716, 724(sh), 738, 755, 784, 796, *826*
dyad **2**	(417)[b] 704, 717, 724(sh), 742, 758, 786, 799, *826*
dyad **3**	(515)[b] 704, 717, 724(sh), 742, 758, 786, 799, *826*
fullerene **7**	700, 716, 724(sh), 738, 755, 784, 796, *826*

[a] Italic numbers indicate fullerene phosphorescence. [b] Pyrazine emission.

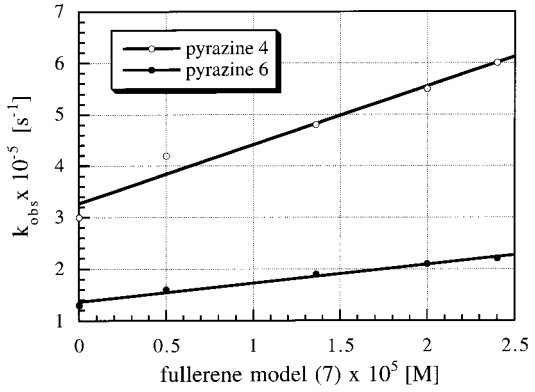

Figure 4. Plot of k_{obs} vs [fullerene **7**] monitored at 420 nm for the energy-transfer process from photoexcited pyrazine **4** (○) and **6** (●) to fullerene model **7** in deoxygenated methylcyclohexane solutions.

Pyrazines 4−6. To probe the excited-state behavior of pyrazine models **4**−**6**, time-resolved differential absorption

spectra were recorded immediately following a 10 ns laser pulse. On the basis of the dominant ground-state absorptions of **4**−**6**, the 355 nm excitation wavelength was chosen. Differential absorption changes following photoexcitation of pyrazines **4**−**6** (4.0×10^{-5} M) in deoxygenated methylcyclohexane show the rapid formation of strong absorption maxima centered around 420 nm. These transient absorptions, with half-lives of 3.5 μs (**4**), 5.2 μs (**5**), and 5.7 μs (**6**), can be ascribed to the triplet excited states of pyrazines.

The difference in excited-state energies between photoexcited monofunctionalized fullerene derivatives with energies of 1.77 eV (^{1}*C_{60})[39] and 1.50 eV (^{3}*C_{60})[39] and the envisaged pyrazine models (ca. 2.6 eV) leads to the assumption that energy transfer might be the predominant deactivation process in dyads **1**−**3**. Therefore, photoexcited pyrazine solutions were subjected to energy-transfer processes with fullerene model **7**. Addition of variable amounts of **7** ($(0.5-2.8) \times 10^{-5}$ M) to methycyclohexane solutions of pyrazines **4**−**6** (4.0×10^{-5} M) resulted in the expected accelerated decay of the pyrazine triplet excited states. The quenching rates were determined from the decay kinetics of the transient absorptions at 420 nm. In all cases, the quenching of the excited states by **7** followed eq 1, where k_{obs} is the observed first-order decay rate constant of the pyrazine excited state, k_d is the rate constant without addition of any fullerene, k_q is the bimolecular quenching rate constant, and [Q] is the quencher concentration (fullerene model **7**):

$$k_{obs} = k_d + k_q[Q] \quad (1)$$

$$^3\text{*(pyrazine)} + \text{fullerene} \rightarrow \text{pyrazine} + {}^3\text{*(fullerene)} \quad (2)$$

The observed first-order rates (k_{obs}) were linearly dependent on the fullerene concentration with intercepts that agreed well with the k_d value obtained in the absence of quencher. The quenching rate constants are 1.1×10^{10} M^{-1} s^{-1} for model **4**, 1.02×10^{10} M^{-1} s^{-1} for model **5**, and 3.64×10^9 M^{-1} s^{-1} for model **6**. Only the last value (**6**) is much lower than those observed for energy-transfer reactions between photoexcited biphenyl ($E_T = 2.80$ eV) and pristine C_{60} or functionalized fullerene derivatives (ca. 1.8×10^{10} M^{-1} s^{-1}).[40] This difference can be related to the driving forces ($\Delta G = E_{pyrazine} - E_{fullerene}$) of the respective energy-transfer reactions. In contrast, the rate constants for pyrazine models **4** and **5** seem to differ only marginally from that reported for biphenyl. Considering a diffusion-controlled rate of 8.8×10^9 M^{-1} s^{-1} in methylcyclohexane (at room temperature),[41] it is safe to assume that the intermolecular energy transfer between the fullerene model and pyrazines **4** and **5** takes place with diffusion-controlled kinetics. More importantly, it should be pointed out that the driving forces for these reactions (**5** ($\Delta G = 1.47$ eV), biphenyl ($\Delta G = 1.3$ eV), **4** ($\Delta G = 1.17$ eV)) are highly exothermic and, thus, support bimolecular kinetics that are either in an "inverted" region or within diffusion-controlled limits.

Further substantiation for the proposed intermolecular energy transfer emerges from the following observation. The fullerene ($T_1 \rightarrow T_n$) characteristics (see further below) and the triplet lifetime differ significantly from those established for photoexcited **4**−**6**. Upon addition of **7**, the visible spectral region revealed a long-lived transient absorption ($\tau_{1/2} = 12$ μs) at 710 nm, which corresponds to the excited triplet states of the fullerene core. The grow-in kinetics of the ($T_1 \rightarrow T_n$) absorption were found to be kinetically linked to the bimolecular deactivation of photoexcited **4**−**6**. This rules out formation of ^{3}*C_{60} via intersystem crossing from the excited singlet state (formed by direct excitation of the C_{60} chromophore). Thus, it is safe to deduce that the bimolecular reaction between excited pyrazines and ground-state fullerenes proceeds via energy transfer, yielding the fullerene's triplet excited state, ^{3}*C_{60}.

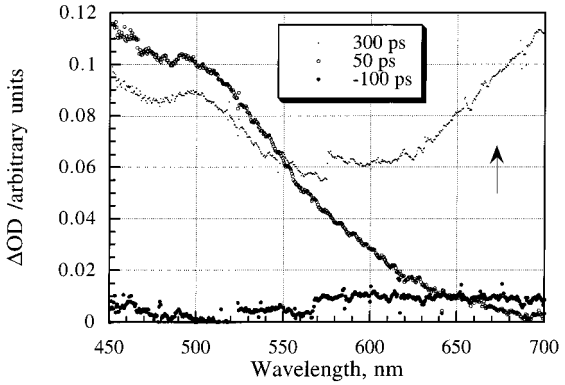

Figure 5. Time-resolved difference absorption spectra of dyad **1** (2.0×10^{-5} M) in deoxygenated methylcyclohexane solution recorded −100, 50, and 300 ps before and after excitation with an 18 ps laser pulse at 355 nm.

Fullerene 7. Transient absorption spectra of **7** (2.0×10^{-5} M) in oxygen-free methylcyclohexane solution revealed the formation of an absorption maximum around 895 nm that is completed around 100 ps after excitation. This resembles the general observation for pristine C_{60} in toluene[42] and is attributed to the excited singlet state (*$S_1 \rightarrow$ *S_n). Its decay follows clean first-order kinetics and results in the formation of a sharp absorption around 710 nm. Since the growth at 710 nm exactly parallels the decay of the singlet absorption, this new band is assigned to the ($T_1 \rightarrow T_n$) absorption. The associated singlet−triplet conversion (ISC) in photoexcited **7** occurs with a half-life of 1.3 ns. It should be noted that, in contrast to pristine C_{60}, functionalization leads to a partial superimposition of the (*$S_1 \rightarrow$ *S_n) and the ($T_1 \rightarrow T_n$) transitions:

$$\text{fullerene} \xrightarrow{h\nu} {}^1\text{*(fullerene)} \xrightarrow{\text{ISC}} {}^3\text{*(fullerene)} \quad (3)$$

Corresponding nanosecond excitation studies were performed with the aim of characterizing the spectral features described above and of further substantiating the formation of fullerene triplet excited states. Nanosecond excitation of a similar solution led to transient absorption bands with λ_{max} at 360 and 710 nm. These spectral characteristics are reminiscent of those reported for the excited triplet states of [6−6]-closed monofunctionalized fullerene derivatives[39] and, furthermore, resemble those observed during the course of the picosecond experiments (see above). Accordingly, the spectral changes can be ascribed to the excited triplet state of **7** evolving from intersystem crossing from the corresponding excited singlet state. The fullerene excited triplet state exhibited a lifetime of 21 μs, leading to the quantitative recovery of the ground state.

Dyads 1−3. The emission quenching of **1**−**3** was investigated by time-resolved studies. Figure 5 shows differential absorption changes of dyad **1** 100 ps before and 50 and 300 ps after picosecond excitation in deoxygenated methylcyclohexane, respectively. Rapid formation of absorptions in the 450−550 nm range is clearly observed. The strong resemblance of the latter with the singlet excited state of **4** leaves little doubt about the excitation of the pyrazine moiety. Despite the spectral similarity, the decay kinetics of the photoexcited pyrazine moiety are distinctly different from those recorded for model **4**. The singlet excited pyrazine moiety is rapidly quenched with $\tau_{1/2} =$ 37 ps (see kinetic time trace at 480 nm, Figure 6) with a deactivation that is qualitatively similar to the grow-in kinetics

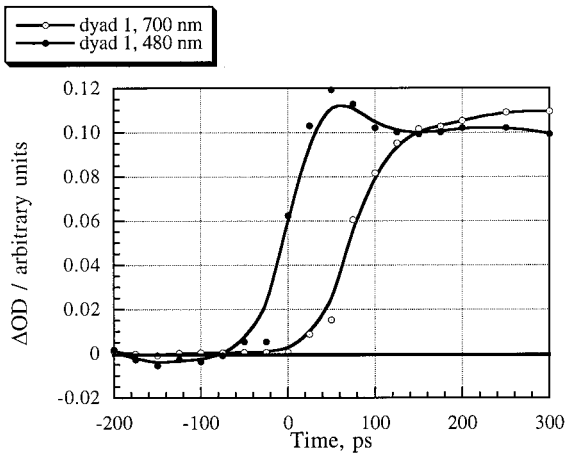

Figure 6. Absorption−time profiles recorded at 700 nm (○) and 480 nm (●) for a deoxygenated methylcyclohexane solution of dyad **1** (2.0×10^{-5} M) following an 18 ps laser pulse at 355 nm.

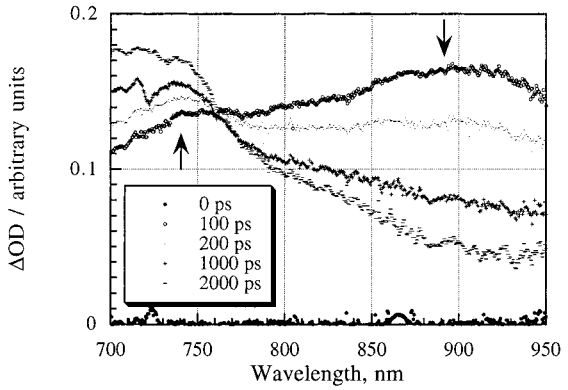

Figure 7. Time-resolved difference absorption spectra of dyad **1** (2.0×10^{-5} M) in deoxygenated methylcyclohexane solution recorded 0, 100, 200, 1000, and 2000 ps after excitation with an 18 ps laser pulse at 355 nm.

of the 700 nm absorption, attributed as above to the strong fullerene ($T_1 \rightarrow T_n$) transition. This substantiates rapid quenching of the pyrazine emission and intramolecular energy transfer to the fullerene triplet state. It should be noted, however, that optical changes in the latter wavelength region evolve also from the fullerene excited singlet state absorptions:

$$\text{pyrazine}-\text{fullerene} \xrightarrow{h\nu} {}^1*(\text{pyrazine})-\text{fullerene} \rightarrow \text{pyrazine}-{}^3*(\text{fullerene}) \quad (4)$$

To dissect the fullerene contribution, the monitored wavelength region was extended into a range of strong ($*S_1 \rightarrow *S_n$)/($T_1 \rightarrow T_n$) transitions and minor pyrazine excited-state absorptions (above 650 nm). Differential transient changes recorded between 700 and 950 nm with different time delays after an 18 ps laser pulse at 355 nm are depicted in Figure 7. The displayed region reveals initial formation of the fullerene excited singlet state absorption centered at 900 nm followed by subsequent deactivation with a half-life of 1.3 ns (the arrow in Figure 7 illustrates the degression of the 900 nm absorption). This decay is parallel to the grow-in of the fullerene ($T_1 \rightarrow T_n$) transition at 700 nm. Furthermore, the ISC process is corroborated by an isosbestic point around 762 nm. This indicates that the presence of the pyrazine moiety does not affect the much slower ISC dynamics of the photoexcited fullerene core. As a consequence of the broadened characteristics, the fullerene ($*S_1 \rightarrow *S_n$) features in dyad **1**−**3** are present, at least in part, in the envisaged 700 nm region (Figure 6).

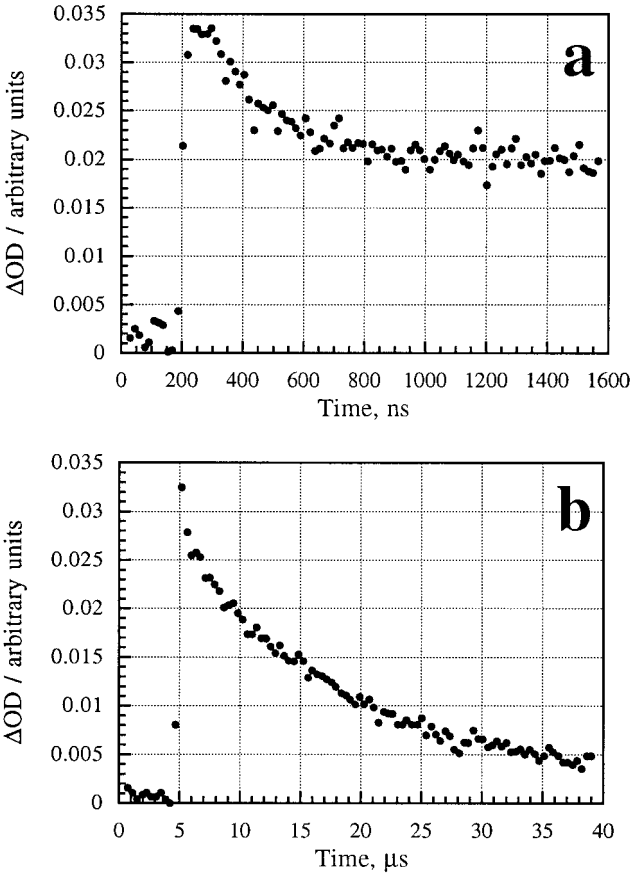

Figure 8. Absorption−time profiles for the decay of the ($T_1 \rightarrow T_n$) transition of photoexcited dyad **3** (at 700 nm) following an 8 ns laser pulse in deoxygenated methylcyclohexane solution.

Picosecond-resolved excitation studies of dyads **2** and **3** led to similar observations. The spectral region around 450 nm shows instaneous formation of the pyrazine singlet excited states. Rapid intramolecular quenching with $\tau_{1/2}$ of 45 and 100 ps was noticed for dyads **2** and **3**, respectively. The lower quenching effectiveness of dyad **3** compared to **1** reflects the differences in bimolecular quenching rates between pyrazine models **4**−**6** and fullerene model **7**.

Nanosecond-resolved experiments under identical conditions were designed to complement the above picosecond studies and to characterize the broad absorption features described above. Spectral changes recorded immediately after an 8 ns pulse indicate two strong absorption bands at 700 and 360 nm. These bands are reminiscent of those described above for fullerene model **7** and correspond to the excited triplet states of the fullerene core. In the absence of oxygen, the fullerene ($T_1 \rightarrow T_n$) absorptions in dyad **1** showed a single-exponential decay and led to clean recovery of the ground state. The lack of any spectral evidence for any other transient intermediate corroborates the emission studies.

In contrast, nanosecond excitation of dyads **2** and **3** in methylcyclohexane resulted in two relaxation processes. The decay of the faster component is virtually completed 1000 ns after the laser pulse with an underlying half-life of 0.22 μs (Figure 8a). The kinetics of the slower decay ($\tau_{1/2} = 14$ μs) reveal a close resemblance to those of fullerene model **7** and dyad **1** (Figure 8b). Differential absorption spectra, taken 100 and 1500 ns after the excitation, are shown in Figure 9. The faster-decaying part is probably due to the fraction that is produced via intramolecular energy transfer from the photoexcited pyrazine. A large photonic energy difference between the

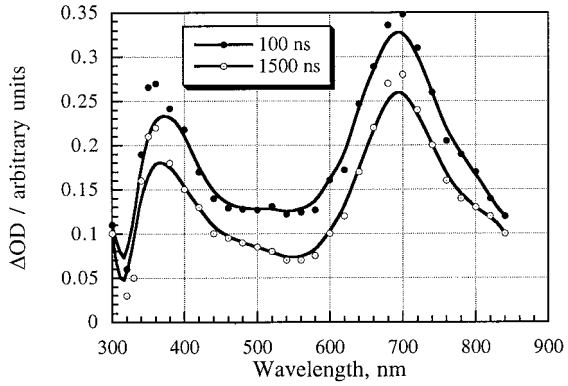

Figure 9. Differential absorption spectra obtained 100 ns (●) and 1500 ns (○) upon flash photolysis at 337 nm of dyad **3** (2.0×10^{-5} M) in deoxygenated methylcyclohexane solution.

excited pyrazine moiety and the fullerene triplet excited state may be responsible, at least in part, for the fast-decaying fullerene triplet excited state. On the other hand, the second component is suggested to evolve from intersystem crossing from the fullerene singlet state, which, in turn, is formed by direct excitation of the fullerene chromophore. It should be noted that variation of the solvent polarity (CH_2Cl_2 and CH_2Cl_2/CH_3CN mixture (1:1 v/v)) had no noticeable effects on the decay dynamics of dyads **1**−**3**.

Finally, the quantum yields of the fullerene excited triplet state in dyads **1**−**3** were determined by the triplet−triplet energy-transfer method using a squarine dye as energy acceptor. The triplet excited state of the fullerene was the donor species, and a crown ether functionalized squarine dye was employed as the acceptor moiety. By comparing the amount of triplet squarine dye formed in each experiment, we were able to determine the triplet quantum yield relative to the triplet quantum yield of pristine C_{60}. Corresponding measurements in deoxygenated methylcyclohexane gave quantum yields near unity, identical to the fullerene model. This corroborates the above emission yields and documents the generation of fullerene excited triplet states in **1**−**3** via two different pathways: (i) direct excitation of the fullerene core and (ii) photoexcitation of the functionalizing pyrazine moieties followed by rapid intramolecular energy-transfer processes from the pyrazine singlet excited state.

Pulse Radiolytic Reduction of Fullerenes. Reduction of the electron-accepting fullerene moieties was probed by another important tool for fast kinetic spectroscopic redox studies, namely, pulse radiolysis under strictly reductive conditions. Radical anions of fullerenes and derivatives such as dyads **1**−**3** can be generated via radiation-induced reduction in solvent mixtures containing toluene/2-propanol/acetone in a 8:1:1 ratio. Toluene has to be used to dissolve dyads **1**−**3** that are practically insoluble in the other two solvents. The reducing species, generated in this solvent mixture, is the radical formed by hydrogen abstraction from 2-propanol and from electron capture of acetone followed by a subsequent protonation ($(CH_3)_2{}^{\bullet}COH$).[43] The experiments (dyads **1**−**3** (2.0×10^{-5})) showed characteristic changes with respect to the formation of the fullerene π-radical anion band in the NIR ($\lambda_{max} = 1040$ nm), which can be regarded as conclusive evidence for reduction of the fullerene core (**1**−**3**). The failure to detect any of those transient absorptions in the NIR during the nanosecond photolysis experiments, however, rules out involvement of any electron-transfer reactions. Furthermore, the lack of electron transfer is in excellent agreement with the high quantum yield of the fullerene excited triplet state.

Formation of Singlet Oxygen. To probe the reactivity of the product from photoexcitation of dyads **1**−**3**, bimolecular quenching rate constants with molecular oxygen were determined from toluene solutions purged with variable amounts of O_2. The oxygen quenching rate constants for **1**−**3** ($(1-1.5) \times 10^9$ M^{-1} s^{-1}) are very similar to those noted for pristine fullerenes and monofunctionalized fullerene derivatives.[3] This suggests that the fullerene-containing dyads generate singlet oxygen quite efficiently via energy transfer:

$$^3*(\text{fullerene}) + O_2 \rightarrow \text{fullerene} + {}^1O_2 \qquad (5)$$

In contrast, pyrazine model **6** gives a much slower reaction (5.0×10^8 M^{-1} s^{-1}) with O_2.

Similarly, reductive quenching of the triplet excited state via electron transfer from sacrificial electron donors such as diazabicyclooctane (DABCO) led to efficient deactivation of the photoexcited fullerene in dyads **1**−**3**. The quenching rate constants ($(5.2-9.4) \times 10^7$ M^{-1} s^{-1}) in toluene are very similar to those reported for monofunctionalized fullerene derivatives.[44] The electron-transfer mechanism was confirmed by applying a solvent with a high dielectric constant, namely, benzonitrile. This solvent is suitable, since it allows not only a reasonable dissolution of dyads **1**−**3** but provides also an environment for a successful charge separation in the reductive quenching process. In the respective experiments, the electron transfer from the electron donor (DABCO) to the photoexcited electron acceptor (fullerene) was detected through the formation of the characteristic fullerene radical anion absorption in the near-IR region ($\lambda_{max} = 1040$ nm).

Conclusion

Functionalization of pristine C_{60} with chromophoric addends, such as the investigated pyrazine derivatives, promotes the UV−vis absorption characteristics of the resulting dyads. Thus, the design of pyrazine−fullerene dyads has been shown to be a versatile approach to improve the light-harvesting efficiency of fullerenes. Intermolecular quenching between triplet excited pyrazine model complexes **4**−**6** and fullerene model **7** leads to efficient energy transfer to the fullerene ground state to generate the fullerene triplet excited state. Similarly, photoexcitation of the pyrazine moieties in dyads **1**−**3** is followed by rapid intramolecular deactivation via energy transfer to the fullerene ground state with half-lives between 37 and 100 ps. In turn, energy transfer transforms the short-lived and moderately redox-active pyrazine singlet excited states into the highly reactive fullerene triplet excited state. The latter is further probed by forming effectively singlet oxygen and undergoing rapid electron transfer with a sacrificial electron donor (DABCO).

Acknowledgment. This work was supported by the Office of Basic Energy Sciences of the U.S. Department of Energy. This is Contribution No. NDRL- 4040 from the Notre Dame Radiation Laboratory. J.M. gratefully acknowledges support by the Bundesministerium für Bildung, Wissenschaft, Forschung und Technologie (BMBF, Bonn) and the Fonds der Chemischen Industrie (Frankfurt). G.G.-T. thanks the European Community (Brussels) for a postdoctoral fellowship (Human Capital and Mobility Program). We are also grateful to Lars Ulmer (Kiel) for the synthesis of pyrazine **5**.

References and Notes

(1) Arbogast, J. W.; Darmanyan, A. P.; Foote, C. S.; Rubin, Y.; Diederich, F. N.; Alvarez, M. M.; Anz, S. J.; Whetten, R. L. *J. Phys. Chem.* **1991**, *95*, 11−12.

(2) Arbogast, J. W.; Foote, C. S.; Kao, M. *J. Am. Chem. Soc.* **1992**, *114*, 2277−2279.
(3) Foote, C. S. *Top. Curr. Chem.* **1994**, *169*, 348−363.
(4) Guldi, D. M.; Asmus, K.-D. *J. Am. Chem. Soc.* **1997**, *119*, 5744−5745.
(5) Ghosh, H. N.; Pal, H.; Sapre, A. V.; Mittal, J. P. *J. Am. Chem. Soc.* **1993**, *115*, 11722−11727.
(6) Alam, M. M.; Watanabe, A.; Ito, O. *J. Photochem. Photobio A* **1997**, *104*, 59−64.
(7) Dimitrijevic, N. M.; Kamat, P. V. *J. Phys. Chem.* **1993**, *97*, 7623−7626.
(8) Hwang, K. C.; Mauzerall, D. *J. Am. Chem. Soc.* **1992**, *114*, 9705−9706.
(9) Niu, S.; Mauzerall, D. *J. Am. Chem. Soc.* **1996**, *118*, 5791−5795.
(10) Hungerbühler, H.; Guldi, D. M.; Asmus, K.-D. *J. Am. Chem. Soc.* **1993**, *115*, 3386-3387.
(11) Bensasson, R. V.; Bienvenue, E.; Dellinger, M.; Leach, S.; Seta, P. *J. Phys. Chem.* **1994**, *98*, 3492−3500.
(12) Diederich, F.; Thilgen, C. *Science* **1996**, *271*, 317−323.
(13) Diederich, F. *Pure Appl. Chem.* **1997**, *69*, 395−400.
(14) Hirsch, A. *The Chemsitry of the Fullerenes*; Georg Thieme Verlag: Stuttgart, 1994.
(15) Prato, M. *J. Mater. Chem.* **1997**, *7*, 1097−1109.
(16) Prato, M.; Maggini, M. *Acc. Chem. Res.*, in press.
(17) Thilgen, C.; Herrmann, A.; Diederich, F. *Angew. Chem., Int. Ed. Engl.* **1997**, *36*, 2268−2280.
(18) Imahori, H.; Sakata, Y. *Adv. Mater.* **1997**, *9*, 537−546.
(19) Jensen, A. W.; Wilson, S. R.; Schuster, D. I. *Bioorg. Med. Chem.* **1996**, *4*, 767−779.
(20) Guldi, D. M.; Maggini, M.; Scoranno, G.; Prato, M. *J. Am. Chem. Soc.* **1997**, *119*, 974−980.
(21) Prato, M.; Maggini, M.; Giacometti, C.; Scorrano, G.; Sandona, G.; Farnia, G. *Tetrahedron* **1996**, *52*, 5221−5234.
(22) Williams, R. M.; Zwier, J. M.; Verhoeven, J. W. *J. Am. Chem. Soc.* **1995**, *117*, 4093−4099.
(23) Williams, R. M.; Koeberg, M.; Lawson, J. M.; An, Y.-Z.; Rubin, Y.; Paddon-Row, M. N.; Verhoeven, J. W. *J. Org. Chem.* **1996**, *61*, 5055−5062.
(24) Thomas, K. G.; Biju, V.; George, M. V.; Guldi, D. M.; Kamat, P. V. *J. Phys. Chem. A*, in press.
(25) Baran, P. S.; Monaco, R. R.; Khan, A. U.; Schuster, D. I.; Wilson, S. R. *J. Am. Chem. Soc.* **1997**, *119*, 8363−8364.
(26) Sariciftci, N. S.; Wudl, F.: Heeger, A. J.; Maggini, M.; Scorrano, G.; Prato, M.; Bourassa, J.; Ford, P. *Chem. Phys. Lett.* **1995**, *247*, 510−514.
(27) Diederich, F.; Dietrich-Buchecker, C.; Nierengarten, J.-F.; Sauvage, J.-P. *J. Chem. Soc., Chem. Commun.* **1995**, 781−782.
(28) Imahori, H.; Yamada, K.; Hasegawa, M.; Taniguchi, S.; Okada, T.; Sakata, Y. *Angew. Chem., Int. Ed. Engl.* **1997**, *36*, 2626−2629.
(29) Imahori, H.; Hagiwara, K.; Aoki, M.; Akiyama, T.; Taniguchi, S.; Okada, T.; Shirakawa, M.; Sakata, Y. *J. Am. Chem. Soc.* **1996**, *118*, 11771−11782.
(30) Kuciauskas, D.; Lin, S.; Seely, G. R.; Moore, A. L.; Moore, T. A.; Gust, D.; Drovetskaya, T.; Reed, C. A.; Boyd, P. D. W. *J. Phys. Chem.* **1996**, *100*, 15926−15932.
(31) Liddell, P. A.; Kuciauskas, D.; Sumida, J. P.; Nash, B.; Nguyen, D.; Moore, A. L.; Moore, T. A.; Gust, D. *J. Am. Chem. Soc.* **1997**, *119*, 1400−1405.
(32) Bell, T. D. M.; Smith, T. A.; Ghiggino, K. P.; Ranasinghe, M. G.; Shepard, M. J.; Paddon-Row, M. N. *Chem. Phys. Lett.* **1997**, *268*, 223−228.
(33) Nakamura, Y.; Minowa, T.; Hayashida, Y.; Tobita, S.; Shizuka, H.; Nishimura, J. *J. Chem. Soc., Faraday Trans.* **1996**, *92*, 377−382.
(34) Kirk, R. E., Othmer, D. E., Eds. *Encyclopedia of Chemical Technology*, 2nd ed.; Interscience: New York; Vol. 2, pp 859−868.
(35) Cheesman, G. W. H.; Werstiuk, E. S. G. *Adv. Heterocycl. Chem.* **1972**, *14*, 99−110.
(36) Porter A. E. A In *Comprehensive Heterocyclic Chemistry*; Katritzky, A. R., Rees C. W., Eds.; Pergamon Press: Oxford 1984; Vol. 3, p 157.
(37) Torres-Garcia, G.; Luftmann, H.; Wolff, C.; Mattay, J. *J. Org. Chem.* **1997**, *62*, 2752−2756.
(38) Ebbesen, T. W. *Rev. Sci. Instrum.* **1988**, *59*, 1307−1309.
(39) Guldi, D. M.; Asmus, K.-D. *J. Phys. Chem. A* **1997**, *101*, 1472−1481.
(40) Dimitrijevic, N. M.; Kamat, P. V. *J. Phys. Chem.* **1992**, *96*, 4811−4814.
(41) Murov, S. L.; Carmichael, I.; Hug, G. L. *Handbook of Photochemistry*; Marcel Dekker: New York, 1993.
(42) Ebbesen, T. W.; Tanigaki, K.; Kuroshima, S. *Chem. Phys. Lett.* **1991**, *181*, 501−504.
(43) Guldi, D. M.; Hungerbühler, H.; Janata, E.; Asmus, K.-D. *J. Phys. Chem.* **1993**, *97*, 11258−11264.
(44) Guldi, D. M.; Hungerbühler, H.; Asmus, K.-D. *J. Phys. Chem.* **1995**, *99*, 9380−9385.